



# Boundary layer flow past a permeable shrinking sheet in a micropolar fluid with a second order slip flow model



Natalia C. Roşca, Ioan Pop\*

Department of Mathematics, Faculty of Mathematics and Computer Science, Babeş-Bolyai University, 400084 Cluj-Napoca, Romania

## ARTICLE INFO

### Article history:

Received 12 March 2014  
Received in revised form  
7 May 2014  
Accepted 16 May 2014  
Available online 23 May 2014

Dedicated to Ahmed Cemal Eringen (born February 15, 1921) the pioneer of micropolar theory

### Keywords:

Micropolar fluid  
Shrinking surface  
Multiple solution  
Numerical solution

## ABSTRACT

Boundary layer flow of a micropolar fluid past a permeable shrinking sheet with second-order slip velocity is studied in this paper. The solution is an exact solution of the Navier–Stokes and microrotation equations. Similarity equations are obtained through the application of similarity transformation techniques. Numerical techniques are used to solve the similarity equations for different values of the shrinking parameter, suction parameter, material parameter and second-order slip parameters. It is shown that the solution has two branches (upper and lower) in a certain range of the parameters. A stability analysis has been also performed to show that the first (upper branch) solutions are stable and physically realizable, while the second (lower branch) solutions are not stable and, therefore, not physically possible. The effects of the governing parameters on the skin friction, velocity and microrotation distribution are presented graphically and discussed. These results clearly show that the second order slip flow model is necessary to predict the flow characteristics accurately.

© 2014 Elsevier Masson SAS. All rights reserved.

## 1. Introduction

Eringen [1] is a pioneering researcher who has formulated about four decades ago the theory of micropolar fluids. It is well known that in many of the real fluids the shear behaviour cannot be characterized by Newtonian relationships and hence researchers have proposed diverse non-Newtonian fluid theories to explain the deviation in the behaviour of real fluids with that of Newtonian fluids. One such theory is that of micropolar fluids. This theory accounts for the internal characteristics of the substructure particles with the assumption that they are allowed to undergo rotation independent of their linear velocity. Micropolar fluids represent fluids consisting of rigid randomly oriented particles suspended in a viscous medium when the deformation of the particles is ignored. The theory of the micropolar fluids can be considered as a generalization of the Navier–Stokes equations. In fact it is a subclass of microfluids, since it takes into account the microstructure of the fluid along with the inertial characteristics of the substructure particles, which are allowed to undergo rotation. Using Eringen's definition on microfluids, a simple microfluid is a fluid medium whose properties and behaviour are strongly influenced by the local motions of the material particles contained in each of

its volume elements. The mathematical background of the micropolar fluid flow theory is presented in the books by Stokes [2], Eringen [3] and Łukaszewicz [4] and in the review papers by Ariman et al. [5,6]. It is pointed out that the theory of micropolar fluids is expected to successfully describe non-Newtonian behaviour of certain fluids, such as liquid crystals, ferro-liquids, colloidal fluids, liquids with polymer additives, animal blood carrying deformable particles (platelets), clouds with smoke, suspensions, slurries, geomorphological sediments, haematological suspensions, etc. The research area of micropolar fluids has been of great interest mainly because the Navier–Stokes equations for Newtonian fluids cannot successfully describe the characteristics of fluid with suspended particles. The equations of motion characterizing a micropolar fluid flow are non-linear in nature (as in the case of Newtonian viscous fluids) and are constituted by a coupled system of vector differential equations in velocity and micro-rotation. Hoyt and Fabula [7] have shown experimentally that fluids containing minute polymeric additives exhibit a considerable reduction in the skin friction (about 25%–30%), a concept which can be explained very well by micropolar fluid theory.

It seems that the concept of boundary layer in micropolar fluids was first introduced by Willson [8] to study the steady, incompressible laminar flow over two-dimensional bodies. Subsequently, the steady boundary-layer flow of micropolar fluids at the stagnation point of a two-dimensional body has been considered by Peddieson and McNitt [9], Nath [10], etc. Several researchers

\* Corresponding author. Tel.: +40 264405300.

E-mail address: [popm.ioan@yahoo.co.uk](mailto:popm.ioan@yahoo.co.uk) (I. Pop).

### Nomenclature

$a$	First-order velocity slip parameter
$b$	Second-order velocity slip parameter
$A, B$	Constants
$c$	Positive constant
$C_f$	Skin friction coefficient
$f(\eta), g(\eta)$	Similarity variables
$j$	Gyration parameter
$K$	Material parameter
$K_n$	Knudsen number
$n$	Constant
$\mathbf{N}$	Microrotation velocity vector
$p$	Pressure
$Re_x$	Local Reynolds number
$s$	Constant suction/injection parameter
$t$	Time
$x$	Coordinate measured along the surface of the sheet
$y$	Coordinate measured normal to the surface of the sheet
$u$	Velocity component along the $x$ -axis
$u_{\text{slip}}$	Slip velocity along the sheet
$u_w(x)$	Stretching/shrinking velocity
$u_e(x)$	External flow velocity
$\mathbf{V}$	Velocity vector
$v$	Velocity component along $y$ -axis
$v_0$	Constant mass flux velocity

### Greek symbols

$\delta$	Molecular mean free path
$\varepsilon$	Momentum accommodation coefficient
$\gamma$	Eigenvalue parameter
$\eta$	Similarity variable
$\kappa$	Vorticity viscosity
$\lambda$	Dimensionless stretching/shrinking parameter
$\lambda_c$	Critical value of $\lambda$
$\mu$	Dynamic viscosity
$\nu$	Kinematic viscosity
$\rho$	Fluid density
$\sigma$	Spin gradient viscosity
$\tau$	Dimensionless time
$\tau_w$	Skin friction or shear stress
$\psi$	Stream function

have considered various stretching problems in micropolar fluids. Ishak et al. [11] investigated on heat transfer over a stretching surface with variable surface heat flux in micropolar fluids. The numerical solution for heat transfer in a micropolar fluid from a non-isothermal stretching sheet with suction and blowing has been studied by Hassanien and Gorla [12], Kelson and Desseaux [13], etc. MHD flow of a micropolar fluid near a stagnation-point towards a non-linear stretching surface has been studied by Hayat et al. [14]. Ahmad et al. [15] studied the unsteady three-dimensional boundary layer flow due to a stretching surface in a micropolar fluid. It should be mentioned to this end that Bhattacharyya et al. [16] have studied the effects of thermal radiation on the steady flow of micropolar fluid and heat transfer past a porous shrinking sheet. Dual solutions of velocity and temperature were obtained for several values of the each parameter involved. For increasing values of the material parameter, the velocity decreases for the first solution, whereas, for the second solution it increases. Due to increase of thermal radiation, the temperature and thermal boundary layer thickness reduce in both solutions and also the heat transfer from the sheet enhances with thermal radiation. Also, in a

very interesting recently published note, Turkyilmazoglu [17] has studied the steady flow of micropolar fluid and heat transfer past a porous shrinking sheet. He has determined mathematically the bounds of multiple existing solutions of purely exponential kind. The presence of dual solutions is proved for the flow field, whose closed-form formulae are then derived. The energy equation is also treated analytically yielding exact solutions beneficial to understand the rate of heat transfer. Also, the very interesting papers by Zheng et al. [18,19] have dealt with dual solutions on micropolar fluids. It is also worth pointing out the published papers on dual and simple solutions by Su et al. [20,21].

In all previous investigations on micropolar fluids past shrinking surfaces, the effects of the second-order slip velocity have been ignored. Therefore, the scope of this paper is to extend the work done by Fang et al. [22] for the boundary layer flow of a viscous fluid over a shrinking sheet with a second-order slip to the case of a shrinking sheet in a micropolar fluid. The partial differential equations are transformed into ordinary (similarity) differential equations, which are then solved numerically. A stability analysis is also performed to show the physically realizable dual solutions. It is shown that the reduced skin friction or the surface shear stress, and the velocity and microrotation profiles due to the shrinking sheet are strongly influenced by the material, mass transfer and the slip flow model parameters. We are confident that the paper is original and the results are completely new and very interesting. It is worth mentioning to this end that, as discussed by Goldstein [23], the shrinking sheet flow is essentially a backward flow and it shows physical phenomena quite distinct from the forward stretching flow.

## 2. Basic equations

Consider the two-dimensional boundary layer flow of a viscous and incompressible micropolar fluid in a quiescent inviscid fluid. In the absence of body forces and body couple, the governing equations are described in vectorial form by, see Hayat et al. [14],

$$\nabla \cdot \mathbf{V} = 0 \quad (1)$$

$$\rho \frac{D\mathbf{V}}{Dt} = -\nabla p + (\mu + \kappa) \nabla^2 \mathbf{V} + \kappa \nabla \times \mathbf{N} \quad (2)$$

$$\rho j \frac{DN}{Dt} = \sigma \nabla^2 \mathbf{N} + \kappa \nabla \times \mathbf{V} - 2 \kappa \mathbf{N} \quad (3)$$

where  $D/Dt$  is the material derivative,  $\mathbf{V}$  is the velocity vector,  $\mathbf{N}$  is the microrotation velocity vector normal to the plane surface and the physical meaning of the other quantities is described in the Nomenclature.

We assume that the surface of the shrinking sheet is located at  $y = 0$  with a fixed end at  $x = 0$ , where  $x$  and  $y$  are the Cartesian coordinates measured along the shrinking surface and in the direction normal to it, respectively, as shown in Fig. 1. It is assumed that the surface is shrunk in the  $x$ -direction with the velocity  $u_w(x)$  and the mass transfer velocity is  $v_0$ , where  $v_0 < 0$  corresponds to the suction and  $v_0 > 0$  to injection or withdrawal of the fluid, respectively.

Under these assumptions Eqs. (1)–(3) can be written in Cartesian coordinates  $x$  and  $y$  as

$$\frac{\partial u}{\partial x} + \frac{\partial v}{\partial y} = 0 \quad (4)$$

$$\begin{aligned} \frac{\partial u}{\partial t} + u \frac{\partial u}{\partial x} + v \frac{\partial u}{\partial y} \\ = -\frac{1}{\rho} \frac{\partial p}{\partial x} + \left( \frac{\mu + \kappa}{\rho} \right) \left( \frac{\partial^2 u}{\partial x^2} + \frac{\partial^2 u}{\partial y^2} \right) + \frac{\kappa}{\rho} \frac{\partial N}{\partial y} \end{aligned} \quad (5)$$

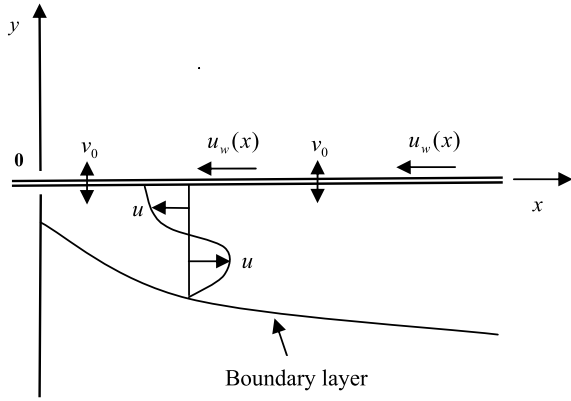


Fig. 1. Physical model and coordinate system for the shrinking sheet.

$$\frac{\partial v}{\partial t} + u \frac{\partial v}{\partial x} + v \frac{\partial v}{\partial y} = -\frac{1}{\rho} \frac{\partial p}{\partial y} + \left(\frac{\mu + \kappa}{\rho}\right) \left(\frac{\partial^2 v}{\partial x^2} + \frac{\partial^2 v}{\partial y^2}\right) - \frac{\kappa}{\rho} \frac{\partial N}{\partial x} \quad (6)$$

$$\frac{\partial N}{\partial t} + u \frac{\partial N}{\partial x} + v \frac{\partial N}{\partial y} = \frac{\sigma}{\rho j} \left(\frac{\partial^2 N}{\partial x^2} + \frac{\partial^2 N}{\partial y^2}\right) + \frac{\kappa}{\rho j} \frac{\partial v}{\partial x} - \frac{\kappa}{\rho j} \left(2N + \frac{\partial u}{\partial y}\right). \quad (7)$$

We shall solve Eqs. (4)–(7) subject to the following initial and boundary conditions:

$$\begin{aligned} t < 0: & \quad v = 0, \quad u = 0, \quad N = 0 \quad \text{for any } x, y, \\ t \geq 0: & \quad v = v_0, \quad u = u_w(x) = \lambda U_w(x) + u_{\text{slip}}(x), \\ & \quad N = -n \frac{\partial u}{\partial y} \quad \text{at } y = 0, \\ & \quad u \rightarrow 0, \quad N \rightarrow 0 \quad \text{as } y \rightarrow \infty \end{aligned} \quad (8)$$

where  $u$  and  $v$  are the velocity components along  $x$  and  $y$  axes,  $\lambda$  is the constant shrinking ( $\lambda < 0$ ) parameter and we assume that  $U_w(x) = cx$ . Further,  $u_{\text{slip}}(x)$  is the slip velocity at the sheet, which is given by Wu [24] and used also by Fang et al. [22], and Fang and Aziz [25],

$$\begin{aligned} u_{\text{slip}}(x) &= \frac{2}{3} \left( \frac{3 - \varepsilon l^2}{\varepsilon} - \frac{3}{2} \frac{1 - l^2}{K_n} \right) \delta \frac{\partial u}{\partial y} \\ &\quad - \frac{1}{4} \left[ l^4 + \frac{2}{K_n^2} (1 - l^2) \right] \delta^2 \frac{\partial^2 u}{\partial y^2} \\ &= A \frac{\partial u}{\partial y} + B \frac{\partial^2 u}{\partial y^2}. \end{aligned} \quad (9)$$

Here  $l = \min(1/K_n, 1)$  and  $\varepsilon$  is the momentum accommodation coefficient with  $0 \leq \varepsilon \leq 1$ . Based on the definition of  $l$ , it is seen that for any given value of  $K_n$ , we have  $0 \leq l \leq 1$ . Since the molecular mean free path  $\delta$  is always positive it results in that  $B$  is a negative number. Further, we notice that  $n$  is a constant such that  $0 \leq n \leq 1$ . The case  $n = 0$ , called strong concentration by Guram and Smith [26], indicates that  $N = 0$  near the surface, represents concentrated particle flows in which the microelements close to the wall surface are unable to rotate (Jena and Mathur, [27]). The case  $n = 1/2$  indicates the vanishing of anti-symmetrical part of the stress tensor and denotes weak concentration (Ahmadi [28]). The case  $n = 1$ , as suggested by Peddieson [29], is used for the modelling of turbulent boundary layer flows. Following Rees and Bassom [30] or Rees and Pop [31], we assume that the spin

gradient  $\sigma$  has the form

$$\sigma = (\mu + \kappa/2)j = \mu(1 + K/2)j \quad (10)$$

where  $K = \kappa/\mu$  is the material parameter.

### 3. Steady-state flow case

We look for a similarity solution of Eqs. (4)–(7) of the form

$$\begin{aligned} \psi &= (cv)^{1/2} xf(\eta), \quad N = c(c/v)^{1/2} xg(\eta), \\ \eta &= (c/v)^{1/2} y \end{aligned} \quad (11)$$

where  $\psi$  is the stream function which is defined in the usual way as  $u = \partial \psi / \partial y$  and  $v = -\partial \psi / \partial x$ . Thus, we have

$$u = cx f'(\eta), \quad v = -\sqrt{cv} f(\eta) \quad (12)$$

where prime denotes differentiation with respect to  $\eta$ . The pressure term can be obtained from Eq. (6) and is given by

$$\frac{p}{\rho} = \frac{\mu + \kappa}{\rho} \frac{\partial v}{\partial y} - \frac{v^2}{2} - \frac{\kappa}{\rho} c \int g(\eta) d\eta + \text{constant}. \quad (13)$$

Substituting (11) into Eqs. (5) and (7), the following set of ordinary differential equations results in

$$(1 + K)f''' + f f'' - f'^2 + K g' = 0 \quad (14)$$

$$(1 + K/2)g'' + f g' - f' g - K(2g + f'') = 0 \quad (15)$$

subject to the boundary conditions

$$\begin{aligned} f(0) &= s, \quad f'(0) = \lambda + a f''(0) + b f'''(0), \\ g(0) &= -n f''(0), \\ f'(\eta) &\rightarrow 0, \quad g(\eta) \rightarrow 0 \quad \text{as } \eta \rightarrow \infty \end{aligned} \quad (16)$$

where  $s = -v_0/\sqrt{cv}$  is the constant parameter of suction ( $s > 0$ ) or injection ( $s < 0$ ),  $a$  is the first order velocity slip parameter with  $a = A\sqrt{c/v} > 0$ ,  $b$  is the second order slip velocity with  $b = Bc/v < 0$  and we take  $j = v/c$ .

The quantity of physical interest is the skin friction coefficient  $C_f$ , which is defined as

$$C_f = \frac{\tau_w}{\rho U_w^2} \quad (17)$$

where  $\tau_w$  is the skin friction or the shear stress along the surface and is given by

$$\tau_w = \left[ (\mu + \kappa) \frac{\partial u}{\partial y} + \kappa N \right]_{y=0}. \quad (18)$$

Substituting (11) into (18) and using (17) we obtain

$$\text{Re}_x^{1/2} C_f = [1 + (1 - n)K] f''(0) \quad (19)$$

where  $\text{Re}_x$  is the local Reynolds number which is defined as  $\text{Re}_x = U_w(x)x/v$ .

It is worth mentioning that for  $K = 0$  and  $\lambda = -1$  (shrinking sheet), Eq. (14) becomes identical with Eq. (7) from the paper by Fang et al. [22]. In fact, for a shrinking sheet in a viscous fluid ( $K = 0$ ) in the absence of the first order ( $a = 0$ ) and second-order ( $b = 0$ ) slip velocity parameters, Eq. (14) reduces to

$$f''' + f f'' - f'^2 = 0 \quad (20)$$

along with the boundary conditions

$$f(0) = s, \quad f'(0) = \lambda, \quad f'(\eta) \rightarrow 0 \quad \text{as } \eta \rightarrow \infty. \quad (21)$$

The exact solution of the boundary value problem (20) and (21) is given by (Vajravelu and Rollings [32] or Cortell [33]),

$$f(\eta) = s + \alpha(1 - e^{-\beta\eta}), \quad (\beta = s + \alpha > 0) \quad (22)$$

where  $\alpha\beta = \lambda$ , from the boundary condition  $f'(0) = \lambda$ . The value  $\beta (> 0)$  is given by the quadratic equation

$$\beta^2 - s\beta - \lambda = 0 \quad (23)$$

and then

$$\beta = \frac{s \pm \sqrt{s^2 + 4\lambda}}{2}. \quad (24)$$

Thus, we have

$$f''(0) = -\frac{\lambda}{2}(s \pm \sqrt{s^2 + 4\lambda}) \quad (25)$$

so that it gives, as it is expected,  $\lambda_c = -s^2/4 < 0$ . Further, we notice that when  $K = 0$  (viscous fluid),  $\lambda = 1$  (stretching sheet) and  $s = 0$  (impermeable surface), we get from (25) that  $f''(0) = -1$ , which is in agreement with the value first reported by Crane [34].

#### 4. Flow stability

Following Weidman et al. [35] or Roşca and Pop [36], we introduce the new dimensionless time variable  $\tau = ct$ . The use of  $\tau$  is associated with an initial value problem and is consistent with the question of which solution will be obtained in practice (physically realizable). Using the variables  $\tau$  and (11), we have

$$\psi = (c\nu)^{1/2}xf(\eta, \tau), \quad u = cx\frac{\partial f}{\partial \eta}(\eta, \tau), \quad (26)$$

$$v = -\sqrt{c\nu}f(\eta, \tau),$$

$$N = c(c/\nu)^{1/2}xg(\eta, \tau), \quad \eta = (c/\nu)^{1/2}y, \quad \tau = ct$$

so that Eqs. (5) and (7) can be written as

$$(1 + K)\frac{\partial^3 f}{\partial \eta^3} + f\frac{\partial^2 f}{\partial \eta^2} - \left(\frac{\partial f}{\partial \eta}\right)^2 + K\frac{\partial g}{\partial \eta} - \frac{\partial^2 f}{\partial \eta \partial \tau} = 0 \quad (27)$$

$$(1 + K/2)\frac{\partial^2 g}{\partial \eta^2} + f\frac{\partial g}{\partial \eta} - \frac{\partial f}{\partial \eta}g - K\left(2g + \frac{\partial^2 f}{\partial \eta^2}\right) - \frac{\partial g}{\partial \tau} = 0 \quad (28)$$

subject to the boundary conditions

$$\begin{aligned} f(0, \tau) &= s, \\ \frac{\partial f}{\partial \eta}(0, \tau) &= \lambda + a\frac{\partial^2 f}{\partial \eta^2}(0, \tau) + b\frac{\partial^3 f}{\partial \eta^3}(0, \tau), \\ g(0, \tau) &= -n\frac{\partial^2 f}{\partial \eta^2}(0, \tau), \\ \frac{\partial f}{\partial \eta}(\eta, \tau) &\rightarrow 0, \quad g(\eta, \tau) \rightarrow 0 \quad \text{as } \eta \rightarrow \infty. \end{aligned} \quad (29)$$

To test stability of the steady flow solution  $f(\eta) = f_0(\eta)$  and  $g(\eta) = g_0(\eta)$  satisfying the boundary-value problem (14)–(16), we write (see Weidman et al. [35] or Roşca and Pop [36]),

$$\begin{aligned} f(\eta, \tau) &= f_0(\eta) + e^{-\gamma\tau}F(\eta, \tau), \\ g(\eta, \tau) &= g_0(\eta) + e^{-\gamma\tau}G(\eta, \tau) \end{aligned} \quad (30)$$

where  $\gamma$  is an unknown eigenvalue parameter, and  $F(\eta, \tau)$  and  $G(\eta, \tau)$  are small relative to  $f_0(\eta)$  and  $g_0(\eta)$ . Substituting (30) into Eqs. (27) and (28), we obtain the following linearized problem

$$\begin{aligned} (1 + K)\frac{\partial^3 F}{\partial \eta^3} + f_0\frac{\partial^2 F}{\partial \eta^2} + (\gamma - 2f_0')\frac{\partial F}{\partial \eta} + f_0''F \\ + K\frac{\partial G}{\partial \eta} - \frac{\partial^2 F}{\partial \eta \partial \tau} = 0 \end{aligned} \quad (31)$$

$$\begin{aligned} (1 + K/2)\frac{\partial^2 G}{\partial \eta^2} + f_0\frac{\partial G}{\partial \eta} + (\gamma - f_0')G + g_0'F - g_0\frac{\partial F}{\partial \eta} \\ - K\left(2G + \frac{\partial^2 F}{\partial \eta^2}\right) - \frac{\partial G}{\partial \tau} = 0 \end{aligned} \quad (32)$$

subject to the boundary conditions

$$\begin{aligned} F(0, \tau) &= 0, \\ \frac{\partial F}{\partial \eta}(0, \tau) &= a\frac{\partial^2 F}{\partial \eta^2}(0, \tau) + b\frac{\partial^3 F}{\partial \eta^3}(0, \tau), \\ G(0, \tau) &= -n\frac{\partial^2 F}{\partial \eta^2}(0, \tau), \\ \frac{\partial F}{\partial \eta}(\eta, \tau) &\rightarrow 0, \quad G(\eta, \tau) \rightarrow 0 \quad \text{as } \eta \rightarrow \infty. \end{aligned} \quad (33)$$

As suggested by Weidman et al. [35], we investigate the stability of the steady flow and heat transfer solution  $f_0(\eta)$  and  $g_0(\eta)$  by setting  $\tau = 0$  and hence  $F = F_0(\eta)$  and  $G = G_0(\eta)$  in (31) and (32) to identify initial growth or decay of the solution (30). To test our numerical procedure we have to solve the linear eigenvalue problem

$$(1 + K)F_0''' + f_0F_0'' + (\gamma - 2f_0')F_0' + f_0''F_0 + K G_0' = 0 \quad (34)$$

$$\begin{aligned} (1 + K/2)G_0'' + f_0G_0' + (\gamma - f_0')G_0 + g_0'F_0 - g_0F_0' \\ - K(2G_0 + F_0'') = 0 \end{aligned} \quad (35)$$

and the boundary conditions (29) become

$$\begin{aligned} F_0(0) &= 0, \quad F_0'(0) = aF_0''(0) + bF_0'''(0), \\ G_0(0) &= -nF_0''(0), \\ F_0'(\eta) &\rightarrow 0, \quad G_0(\eta) \rightarrow 0 \quad \text{as } \eta \rightarrow \infty. \end{aligned} \quad (36)$$

It should be mentioned that for particular values of  $K, s, n, a, b$  and  $\lambda$  the stability of the corresponding steady flow solution  $f_0(\eta)$  and  $g_0(\eta)$  is determined by the smallest eigenvalue  $\gamma$ . According to Harris et al. [37], the range of possible eigenvalues can be determined by relaxing a boundary condition on  $F_0(\eta)$  and  $G_0(\eta)$ . For the present problem, we relax the condition that  $G_0(\eta) \rightarrow 0$  as  $\eta \rightarrow \infty$  and for a fixed value of  $\gamma$  we solve Eqs. (34) and (35) along with the new boundary condition (36) and  $G_0'(0) = 1$ .

#### 5. Numerical method

Following Roşca and Pop [36] numerical solutions to the nonlinear ordinary differential equations (14) and (15) with the boundary conditions (16) are obtained using the function `bvp4c` from Matlab for different values of the material parameter  $K$ , suction  $s$ , and several values of the constants  $n, a$  (first-order) and  $b$  (second-order) slip velocity parameters when  $\lambda < 0$  (shrinking sheet). The code `bvp4c` is based on a three-stage collocation at Lobatto points, hence it is equivalent to the three-stage Lobatto IIIA method. Lobatto IIIA methods have been considered for boundary value problems due to their very good stability properties and they have fourth-order accuracy over the whole interval. In this approach, the differential equations are first reduced to a system of first-order equations

**Table 1**  
Comparison of  $f''(0)$  for several values of  $s$ ,  $a$  and  $b$  when  $K = 0$  and  $\lambda = -1$  (shrinking sheet).

$s$	$a$	$b$	Present study		Fang et al. [22]	
			Upper branch	Lower branch	Upper branch	Lower branch
2	0.5	-1	0.3412	0.3159	0.3412	0.3159
	0.5	-2	0.2038	0.2656	0.2038	0.2656
	1	-1	0.2905	0.2565	0.2905	0.2565
	1	-2	0.1846	0.2257	0.1847	0.2257
3	0.5	-1	0.2627	0.2413	0.2629	0.2413
	0.5	-2	0.1470	0.2173	0.1469	0.2173
	1	-1	0.2320	0.2022	0.2317	0.2022
	1	-2	0.1369	0.1869	0.1371	0.1868

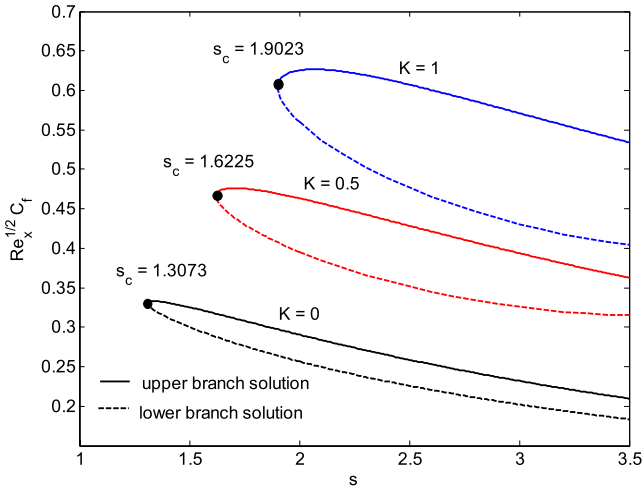


**Fig. 2.** Variation of  $Re_x^{1/2} C_f$  with  $s$  for several values of  $K$  when  $n = 0.2$ ,  $a = 1$ ,  $b = -1$ ,  $\lambda = -1$ .

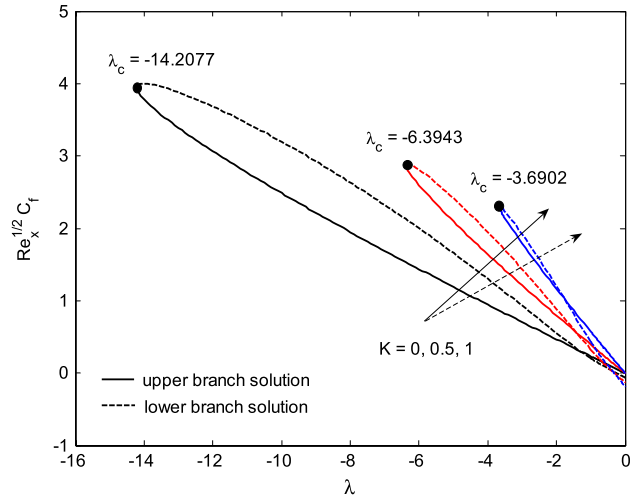


**Fig. 4.** Variation of  $Re_x^{1/2} C_f$  with  $\lambda$  for several values of  $K$  when  $n = 0.2$ ,  $a = 1$ ,  $b = -1$ ,  $s = 3$ .

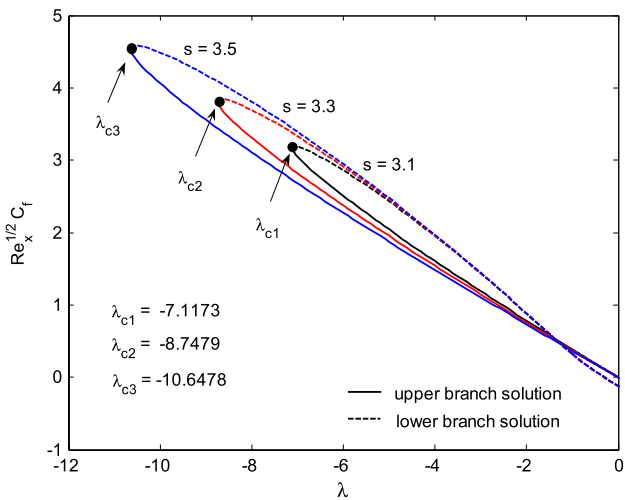


**Fig. 3.** Variation of  $Re_x^{1/2} C_f$  with  $\lambda$  for several values of  $s$  when  $K = 0.5$ ,  $n = 0.2$ ,  $a = 1$ ,  $b = -1$ .

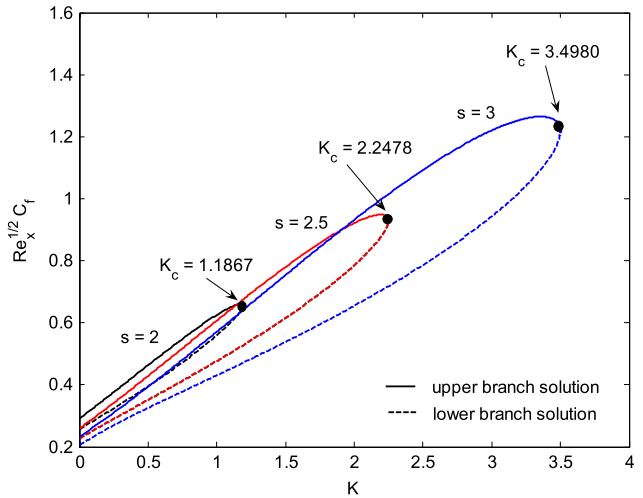


**Fig. 5.** Variation of  $Re_x^{1/2} C_f$  with  $K$  for several values of  $s$  when  $n = 0.2$ ,  $a = 1$ ,  $b = -1$ ,  $\lambda = -1$ .

by introducing new variables. The mesh selection and error control are based on the residual of the continuous solution. The relative tolerance was set to  $10^{-7}$  and the boundary layer thickness  $\eta = \eta_\infty$  has to be determined in order to apply the far field boundary conditions (16). It is found that the value  $\eta = \eta_\infty = 20$  for the upper branch solution and  $\eta = \eta_\infty$  in the range 40–120 for the lower branch solution are adequate for all velocity and microrotation velocity profiles to satisfy the infinity boundary conditions (16) asymptotically. Examples of solving boundary value problems by bvp4c code can be found in the book by Shampine et al. [38] or through online tutorial by Shampine et al. [39].

**6. Results and discussion**

Table 1 shows the comparison values of  $f''(0)$  obtained solving numerically Eq. (14) with those reported by Fang et al. [22] for some values of  $s$ ,  $a$  and  $b$  when  $K = 0$  (classical viscous fluid) and  $\lambda = -1$  (shrinking sheet). It is seen that the comparison is in very good agreement, and thus gives confidence to the accuracy of the numerical results.

Further, the values of the local skin friction coefficient  $Re_x^{1/2} C_f$  are shown in Figs. 2–8 for some values of the suction parameter  $s$  ( $>0$ ), material parameter  $K$  and for some values of  $a$  and  $b$

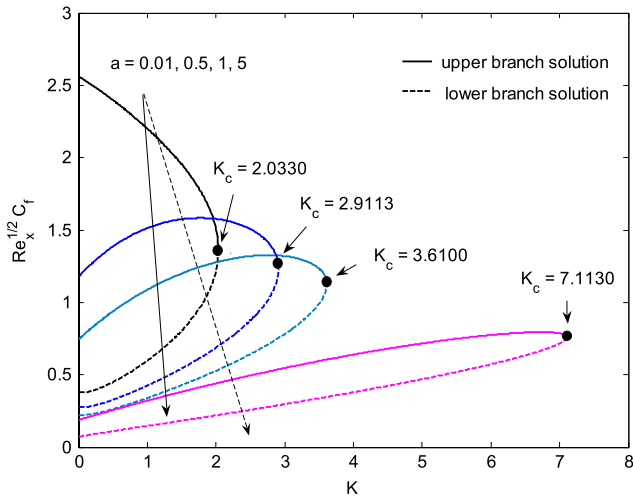


Fig. 6. Variation of  $Re_x^{1/2} C_f$  with  $K$  for several values of  $a$  when  $n = 0.2$ ,  $b = 0$ ,  $s = 3$ ,  $\lambda = -1$ .

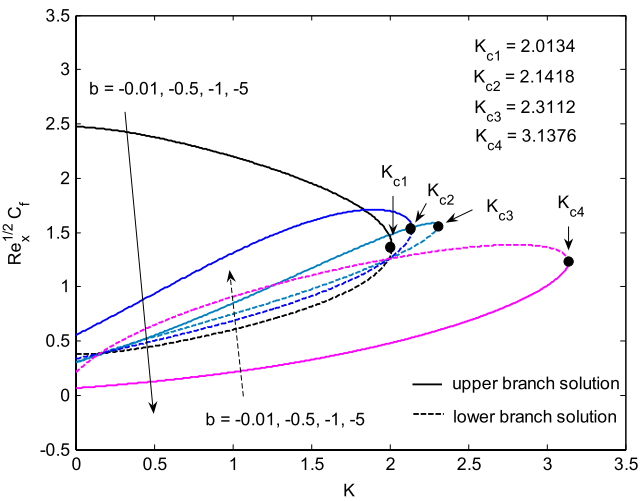


Fig. 7. Variation of  $Re_x^{1/2} C_f$  with  $K$  for several values of  $b$  when  $n = 0.2$ ,  $a = 0$ ,  $s = 3$ ,  $\lambda = -1$ .

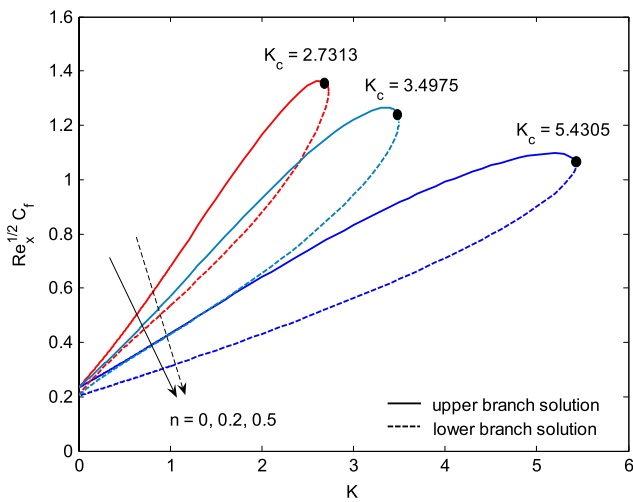


Fig. 8. Variation of  $Re_x^{1/2} C_f$  with  $K$  for several values of  $n$  when  $a = 1$ ,  $b = -1$ ,  $s = 3$ ,  $\lambda = -1$ .

Table 2

Smallest eigenvalues  $\gamma$  at several values of  $s$ ,  $K$  and  $\lambda$  when  $n = 0.2$ ,  $a = 1$  and  $b = -1$ .

$s$	$K$	$\lambda$	Upper branch $\gamma$	Lower branch $\gamma$
2	0.3	-2.10	0.3580	-0.3326
		-2.20	0.2642	-0.2508
		-2.30	0.1015	-0.0995
	0.5	-2.31	0.0660	-0.0651
		-1.60	0.3714	-0.3375
		-1.70	0.2747	-0.2569
3	0.5	-1.80	0.1064	-0.1034
		-1.81	0.0700	-0.0685
		-6.00	0.5772	-0.5517
	1	-6.20	0.4057	-0.3934
		-6.30	0.2825	-0.2766
		-6.39	0.0603	-0.0600
1	-3.40	0.5442	-0.5119	
	-3.50	0.4412	-0.4203	
	-3.60	0.3037	-0.2939	
		-3.69	0.0137	-0.0140

(lower branch) solutions. The value of  $g(0)$  will not be given because  $g(0) = -nf''(0)$ . It is to be noticed from Fig. 2 that the values of  $Re_x^{1/2} C_f$  increase as both suction parameter  $s$  ( $>0$ ) and the material parameter  $K$  increase. The suction parameter is very significant in maintaining the steady boundary layer near the sheet by delaying the separation. In accordance with the results presented in the paper by Fang et al. [22] for a permeable shrinking sheet, dual solutions occur only when the suction parameter  $s$  takes moderate values, namely  $s \geq 1.3073$  for the present problem and it results in a critical value  $s = s_c(K)$ . There are two solutions when  $s > s_c$ , one solution when  $s = s_c$  and no solution when  $s < s_c$ , where  $s_c$  the critical value of  $s$  for which the solution exists. It should be mentioned that for  $s < s_c$  the ordinary differential equations (14)–(16) have no solutions and the full Navier–Stokes and microrotation equations should be solved.

Figs. 3 and 4 illustrate the variation of  $Re_x^{1/2} C_f$  with  $\lambda < 0$ , while Figs. 5–8 show the variation of  $Re_x^{1/2} C_f$  with  $K$  for several values of the parameters  $s$ ,  $n$ ,  $a$  and  $b$ . These figures also show that the dual (upper and lower branch) solutions to the similarity equations (14)–(16) depend on the parameters  $K$ ,  $s$ ,  $n$ ,  $a$  and  $b$ . As for the classical fluids ( $K = 0$ ) the critical values  $|\lambda_c|$  increase as  $s$  and  $K$  increase. Further, it can be seen that there exist values  $K_c (>0)$  of  $K$  up to which dual solutions occur. The values of  $K_c$  increase when the parameters  $s$ ,  $n$ ,  $a$  and  $b$  increase. For  $K > K_c$  the ordinary differential equations (14)–(16) have no solutions and the full Navier–Stokes and microrotation equations have to be solved. From the stability analysis presented, it can be seen that the upper branch solutions are stable and physically realizable, while the lower branch solutions are unstable and, therefore, not physically realizable. The smallest eigenvalues  $\gamma$  at several values of the parameters  $K$ ,  $s$ ,  $n$ ,  $a$ ,  $b$  and  $\lambda$  are given in Table 2.

Finally, the effects of the parameters  $K$ ,  $s$  and  $\lambda$  on the velocity  $f'(\eta)$  and microrotation  $g(\eta)$  profiles are presented in Figs. 9–14. Similar to Figs. 2–8, the far field boundary conditions (16) are satisfied asymptotically, which supports the validity of the numerical results obtained. It is observed from Figs. 9–14 that there are two profiles for particular values of the parameters  $K$ ,  $s$  and  $\lambda$ , while the other parameters are fixed. Further, it is clearly seen from these figures that for the velocity and microrotation profiles, the first solutions display a thinner boundary layer thickness compared to the second solutions. Therefore, it is supported the validity of the numerical results obtained and the existence of the dual solutions given in Figs. 2–8. It is also worth mentioning that for several values of the suction parameter  $s$ , the velocity  $f'(\eta)$  and microrotation  $g(\eta)$  profiles given in Figs. 9 and 10 are similar with the ones illustrated in Fig. 2((a), (b)) in the paper by Turkyilmazoglu [17].

when  $\lambda < 0$  (shrinking sheet) and  $n = 0.2$ . It is seen that dual solutions of Eqs. (14)–(16) exist, first (upper branch) and second

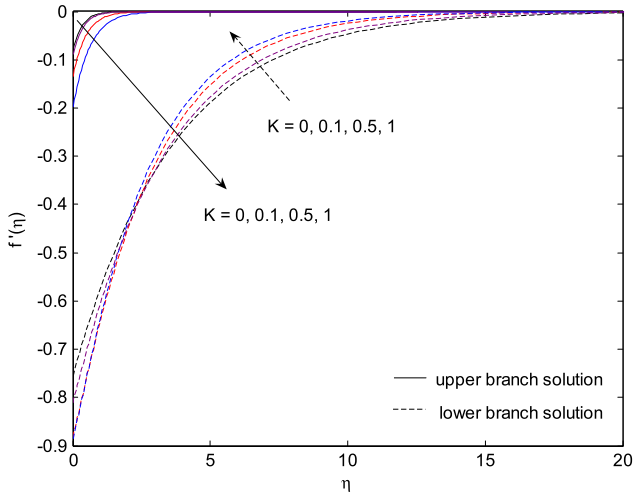


**Fig. 9.** Dimensionless velocity  $f'(\eta)$  profiles for several values of  $K$  when  $n = 0.2$ ,  $a = 1$ ,  $b = -1$ ,  $s = 3$ ,  $\lambda = -1$ .

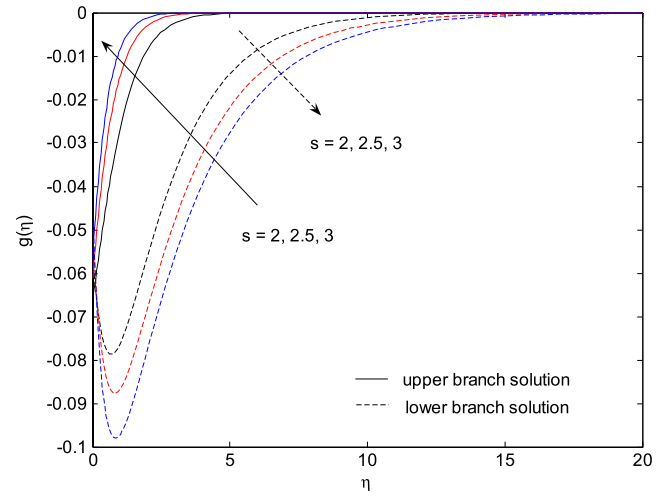


**Fig. 12.** Dimensionless microrotation  $g(\eta)$  profiles for several values of  $s$  when  $K = 0.5$ ,  $n = 0.2$ ,  $a = 1$ ,  $b = -1$ ,  $\lambda = -1$ .

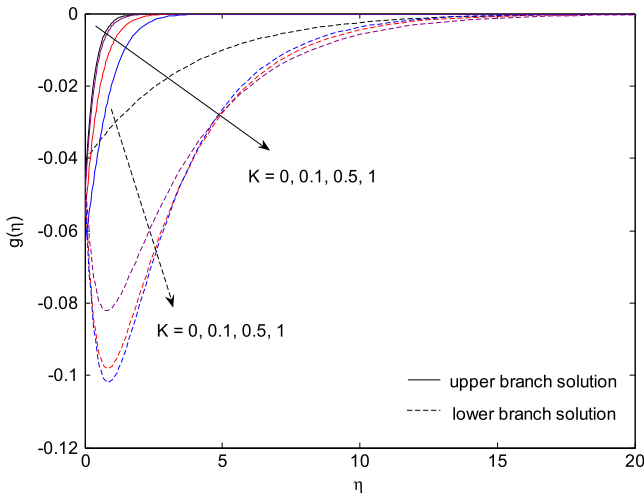


**Fig. 10.** Dimensionless microrotation  $g(\eta)$  profiles for several values of  $K$  when  $n = 0.2$ ,  $a = 1$ ,  $b = -1$ ,  $s = 3$ ,  $\lambda = -1$ .

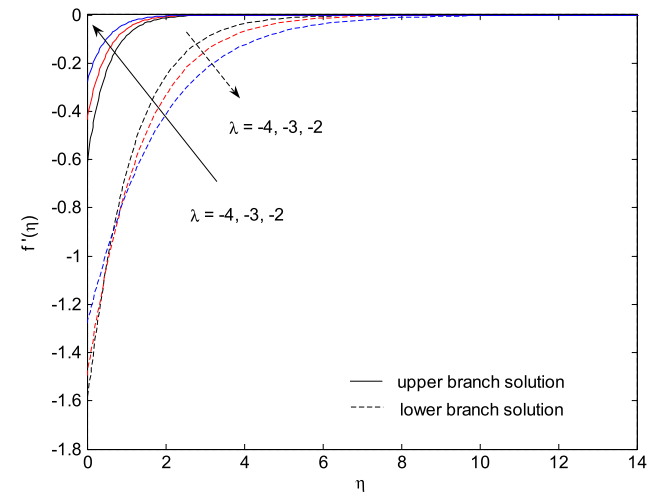


**Fig. 13.** Dimensionless velocity  $f'(\eta)$  profiles for several values of  $\lambda$  when  $K = 0.5$ ,  $n = 0.2$ ,  $a = 1$ ,  $b = -1$ ,  $s = 3$ .

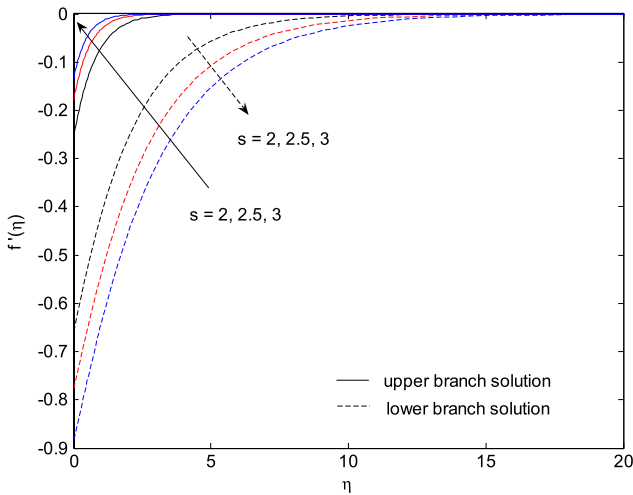


**Fig. 11.** Dimensionless velocity  $f'(\eta)$  profiles for several values of  $s$  when  $K = 0.5$ ,  $n = 0.2$ ,  $a = 1$ ,  $b = -1$ ,  $\lambda = -1$ .

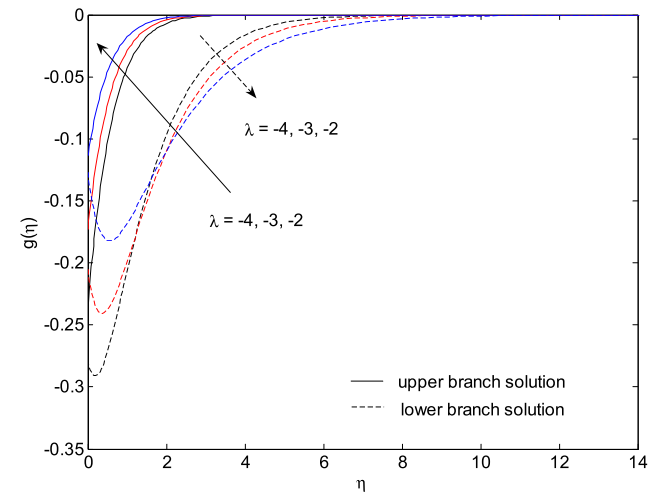


**Fig. 14.** Dimensionless microrotation  $g(\eta)$  profiles for several values of  $\lambda$  when  $K = 0.5$ ,  $n = 0.2$ ,  $a = 1$ ,  $b = -1$ ,  $s = 3$ .

## 7. Conclusions

A theoretical study has been presented for the boundary layer flow of a micropolar fluid over a permeable shrinking sheet under the second-order slip velocity condition. By means of such a treatment, it is shown to be possible to explore the physical features of the flow and microrotation characteristics. By solving two coupled similarity equations (14) and (15) subject to the boundary conditions (16), it is found that no solution or at most two (dual, upper and lower branch) solutions may exist depending on the working parameters considered in the physical model, namely, shrinking parameter  $\lambda$  ( $<0$ ), suction parameter ( $s > 0$ ), material parameter  $K$  and second-order slip parameters  $a$  ( $>0$ ) and  $b$  ( $<0$ ). The range of critical values  $s_c$  increases with the increase of  $K$  for which the solutions exist. The material parameter  $K$  increases the range of the critical parameter  $|\lambda_c|$  for which the solutions exist. The values of  $K$  increase the skin friction coefficient  $Re_x^{1/2} C_f$  for the upper branch solutions, while  $K$  decreases  $Re_x^{1/2} C_f$  for the lower branch solutions.

## Acknowledgements

The authors wish to express their thanks to the very competent Reviewers for the valuable comments and suggestions.

## References

- [1] A.C. Eringen, Theory of micropolar fluids, *J. Math. Mech.* 16 (1996) 1–18.
- [2] V.K. Stokes, *Theories of Fluids with Microstructures*, Springer, New York, 1984.
- [3] A.C. Eringen, *Microcontinuum Field Theories: II* Fluent Media, Springer, New York, 2001.
- [4] G. Łukasiewicz, *Micropolar Fluids: Theory and Application*, Birkhäuser, Boston, 1984.
- [5] T. Ariman, M.A. Turk, N.D. Sylvester, Microcontinuum fluids mechanics-a review, *Internat. J. Engrg. Sci.* 11 (1973) 905–930.
- [6] T. Ariman, M.A. Turk, N.D. Sylvester, Application of microcontinuum fluid mechanics, *Internat. J. Engrg. Sci.* 12 (1974) 273–293.
- [7] J.W. Hoyt, A.G. Fabula, *The Effect of Additives on Fluid Friction*. US Naval Ordinance Test Station Report, USA, 1964.
- [8] A.G. Willson, Boundary layers in micropolar fluids, *Proc. Cambridge Philos. Soc.* 67 (1970) 469–476.
- [9] J.R.J. Peddieson, R.P. McNitt, Boundary-layer theory for a micropolar fluid, *Recent Adv. Eng. Sci.* 5 (1970) 405–476.
- [10] G. Nath, Similar solutions for the incompressible laminar boundary layer with pressure gradient in micropolar fluids, *Rheol. Acta* 14 (1975) 850–857.
- [11] A. Ishak, R. Nazar, I. Pop, Heat transfer over a stretching surface with variable surface heat flux in micropolar fluids, *Phys. Lett. A* 372 (2008) 559–561.
- [12] I.A. Hassanien, R.S.R. Gorla, Heat transfer to a micropolar fluid from a non-isothermal stretching sheet with suction and flowing, *Acta Mech.* 84 (1990) 191–199.
- [13] N.A. Kelson, A. Desseaux, Effect of surface conditions on flow of a micropolar fluid driven by a porous stretching sheet, *Internat. J. Engrg. Sci.* 39 (2001) 1881–1897.
- [14] T. Hayat, T. Javed, Z. Abbas, MHD flow of a micropolar fluid near a stagnation-point towards a non-linear stretching surface, *Nonlinear Anal. RWA* 10 (2009) 1514–1526.
- [15] S. Ahmad, R. Nazar, A. Ishak, I. Pop, Unsteady three-dimensional boundary layer flow due to a stretching surface in a micropolar fluid, *Internat. J. Numer. Methods Fluids* 68 (2012) 1561–1573.
- [16] K. Bhattacharyya, S. Mukhopadhyay, G.C. Layek, I. Pop, Effects of thermal radiation on micropolar fluid flow and heat transfer over a porous shrinking sheet, *Int. J. Heat Mass Transfer* 55 (2012) 2945–2952.
- [17] M. Turkyilmazoglu, A note on micropolar fluid flow and heat transfer over a porous shrinking sheet, *Int. J. Heat Mass Transfer* 72 (2014) 388–391.
- [18] L. Zheng, J. Niu, X. Zhang, L. Ma, Dual solutions for flow and radiative heat transfer of a micropolar fluid over stretching/shrinking sheet, *Int. J. Heat Mass Transfer* 55 (2012) 7577–7586.
- [19] L. Zheng, N. Liu, J. Niu, X. Zhang, Slip and buoyancy lift effects on the mixed flow and radiation heat transfer of a micropolar fluid towards vertical permeable plate, *J. Porous Media* 16 (2013) 031705.
- [20] X. Su, L. Zheng, X. Zhang, DTM-BF method and dual solutions for an unsteady MHD flow over a permeable shrinking sheet with velocity slip, *Appl. Math. Mech. (English Ed.)* 33 (2012) 1555–1568.
- [21] X. Su, L. Zheng, X. Zhang, J. Zhang, MHD mixed convective heat transfer over a permeable stretching wedge with thermal radiation and ohmic heating, *Chem. Eng. Sci.* 78 (2012) 1–8.
- [22] T. Fang, S. Yao, J. Zhang, A. Aziz, Viscous flow over a shrinking sheet with a second order slip flow model, *Commun. Nonlinear Sci. Numer. Simul.* 15 (2010) 1831–1842.
- [23] S. Goldstein, On backward boundary layers and flow in converging passages, *J. Fluid Mech.* 21 (1965) 33–45.
- [24] L. Wu, A slip model for rarefied gas flows at arbitrary Knudsen number, *Appl. Phys. Lett.* 93 (2008) 253103. (3 pages).
- [25] T. Fang, A. Aziz, Viscous flow with second-order slip velocity over a stretching sheet, *Z. Nat.forsch. A* 65a (2010) 1087–1092.
- [26] G.S. Gura, C. Smith, Stagnation flows of micropolar fluids with strong and weak interactions, *Appl. Math. Comput.* 6 (1980) 213–233.
- [27] S.K. Jena, M.N. Mathur, Similarity solutions for laminar free convection flow of a thermomicropolar fluid past a nonisothermal flat plate, *Internat. J. Engrg. Sci.* 19 (1981) 1431–1439.
- [28] G. Ahmadi, Self-similar solution of incompressible micropolar boundary layer flow over a semi-infinite plate, *Internat. J. Engrg. Sci.* 14 (1976) 639–646.
- [29] J. Peddieson, An application of the micropolar fluid model to the calculation of turbulent shear flow, *Internat. J. Engrg. Sci.* 10 (1972) 23–32.
- [30] D.A.S. Rees, A.P. Bassom, The Balmus boundary-layer flow of a micropolar fluid, *Internat. J. Engrg. Sci.* 34 (1996) 113–124.
- [31] D.A.S. Rees, I. Pop, Free convection boundary-layer flow of a micropolar fluid from a vertical flat plate, *IMA J. Appl. Math.* 61 (1998) 179–197.
- [32] K. Vajravelu, D. Rollins, Hydromagnetic flow of a second grade fluid over a stretching sheet, *Appl. Math. Comput.* 148 (2004) 783–791.
- [33] R. Cortell, Viscous flow and heat transfer over a nonlinearly stretching sheet, *Appl. Math. Comput.* 184 (2007) 864–873.
- [34] L.J. Crane, Flow past a stretching plate, *J. Appl. Math. Phys. (ZAMP)* 21 (1970) 645–647.
- [35] P.D. Weidman, D.G. Kubitschek, A.M.J. Davis, The effect of transpiration on self-similar boundary layer flow over moving surfaces, *Internat. J. Engrg. Sci.* 44 (2006) 730–737.
- [36] N.C. Roşca, I. Pop, Mixed convection stagnation point flow past a vertical flat plate with a second order slip: heat flux case, *Int. J. Heat Mass Transfer* 65 (2013) 102–109.
- [37] S.D. Harris, D.B. Ingham, I. Pop, Mixed convection boundary-layer flow near the stagnation point on a vertical surface in a porous medium: Brinkman model with slip, *Transp. Porous Media* 77 (2009) 267–285.
- [38] L.F. Shampine, I. Gladwell, S. Thompson, *Solving ODEs with MATLAB*, Cambridge University Press, 2003.
- [39] L.F. Shampine, M.W. Reichelt, J. Kierzenka, *Solving boundary value problems for ordinary differential equations in Matlab with bvp4c*, 2010. [http://www.mathworks.com/bvp\\_tutorial](http://www.mathworks.com/bvp_tutorial).